

# An Evaluation of Bulk Ri-Based Surface Layer Flux Formulas for Stable and Very Stable Conditions with Intermittent Turbulence

GREGORY S. POULOS

*Colorado Research Associates, NWRA, Boulder, Colorado*

SEAN P. BURNS

*National Center for Atmospheric Research, Boulder, Colorado*

(Manuscript received 29 July 2002, in final form 7 February 2003)

## ABSTRACT

High-rate near-surface overnight atmospheric data taken during the Cooperative Atmosphere–Surface Exchange Study-1999 (CASES-99) is used to quantify the representativeness of surface layer formulations under statically stable conditions. Combined with weak wind shear, such conditions generate large dynamic stability ( $Ri > 1.0$ ), intermittency, and nonstationarity, which violate the underlying assumptions of surface layer theory. Still, such parameterizations are applied in atmospheric numerical models from large-eddy to global circulation.

To investigate two formulas, their parameterized sensible heat flux and friction velocity ( $u_*$ ) values are compared, when driven by CASES-99 measurements, to CASES-99 measurements of the same from various heights. Significant inaccuracies in the magnitude and sign of flux are found with 1) a frequent, large underprediction of heat flux for  $Ri_b > \sim 1.0$ , 2) an overprediction of negative sensible heat flux and  $u_*$  for  $\sim 0.2 < Ri_b < \sim 0.8$ , 3) a systematic underprediction of  $u_*$  for  $Ri_b > 1.0$  for one of the schemes tested, and 4) a misrepresentation of natural heat and  $u_*$  intermittency by both schemes for  $Ri > \sim 1.0$ . Failures of the “constant flux assumption” for a given height are proposed as a partial source for the errors. Using experimental data, a surface layer of  $\mathcal{O}[1\text{--}10]$  m is found during dynamically stable conditions. Rather than suggest a revised algebraic fit to the observations, an alternate approach to surface layer parameterization is proposed.

## 1. Introduction

This study is motivated by the generally large number of outstanding questions regarding atmospheric behavior in the nocturnal boundary layer (NBL), and particularly the dynamically stable NBL (Nappo and Johansson 1998; Hunt et al. 1996; Carson and Richards 1978; Mahrt 1999). The Cooperative Atmosphere–Surface Exchange Study-1999 (CASES-99) field program, in partially addressing these questions, attempted to identify the sources and to quantify the physical characteristics of atmospheric phenomena occurring from the formative stages of the NBL until its eventual breakup during the morning transition (Poulos et al. 2002). Included among the four CASES-99 scientific goals is the desire “to measure heat and momentum fluxes and their divergences accompanying the events contributing to turbulence, transports, and mixing throughout the nocturnal boundary layer, and especially within the surface layer ( $\sim 10$  to  $20$  m), to assess the departures from similarity theory under weakly stable and very stable con-

ditions” (Poulos et al. 2002). This scientific goal lays the foundation for investigations of parameterization problems in numerical models, including large-eddy simulation (e.g., Wyngaard and Peltier 1996; Saiki et al. 2000; Kosovic and Curry 2000), mesoscale models (e.g., Hanna and Yang 2001; Belair et al. 1998; Poulos 1996), and larger-scale models (e.g., Bhumralkar 1975; Louis 1982; Mahrt 1999). The eventual improvement of parameterizations in this regard is presumed to have a significant impact on nocturnal temperature prediction, representation of vertical structure of stratification and consequent daytime convective boundary layer (CBL) growth, and constituent dispersion in stably stratified conditions (Oetl et al. 2001).

### *a. Similarity assumptions in the atmospheric surface layer*

Problems are frequently encountered by numerical models attempting to simulate near-surface atmospheric evolution under stably stratified nocturnal conditions (Holtslag and De Bruin 1988; Beljaars and Holtslag 1991; McNider et al. 1995; Derbyshire 1999). Most numerical models depend, in the surface layer (inasmuch as it is defined for the NBL), on similarity theory–based

---

*Corresponding author address:* Gregory S. Poulos, Colorado Research Associates, NWRA, 3380 Mitchell Lane, Boulder, CO 80301.  
E-mail: gsp@cora.nwra.com

parameterizations (e.g., McVehil 1964; Webb 1970; Businger et al. 1971; Louis 1979; Kot and Song 1998), although a variety of approaches have been attempted (Pleune 1990; Herbert and Panhans 1979; Hartel and Kleiser 1998; Dubrulle et al. 2002a,b). However, as discussed by Mahrt (1998b, 1999), the stably stratified atmospheric surface fluxes are not adequately described by existing Monin–Obukhov similarity theory, which is more appropriately applied to the weakly stable, neutral, and convective boundary layers or where  $Ri < \sim 0.2$  (Nieuwstadt 1984; Derbyshire 1994, 1995; Hill 1997; Mahrt et al. 1998). Still, this theory is applied in modern numerical weather prediction models (Chen et al. 1997).

Formulating surface fluxes when dynamic stability is high is made difficult by the fact that the NBL is often characterized by intermittent turbulent bursts of  $O[10]$  to  $O[1000]$  s (e.g., Businger 1973; Schubert 1977; Coulter 1990; Blumen et al. 2001). These sporadic or episodic events that populate the nighttime stable boundary layer (Nappo 1991; Mahrt 1999; Mahrt et al. 1998; Howell and Sun 1997; Blumen et al. 2001) do not lead to statistically steady-state turbulence, which underlies one of the major assumptions of existing theory. Other studies have shown that intermittent bursts of turbulence and mixing can also occur multiple times on a given night (Finnigan 1979; De Baas and Driedonks 1985; Weber and Kurzeja 1991; Katul et al. 1994; Finnigan 1999; Coulter and Doran 2002; Sun et al. 2002). Such behavior is verified by the detailed clear-sky nighttime measurements taken during CASES-99 over quite flat terrain. Contributions to intermittent turbulence have been found from nonlocal turbulence sources such as density currents, solitary waves, roll vortices, Kelvin–Helmholtz billows, elevated ducted waves, multiscale katabatic flows, residual layer turbulence downward penetration, physiographic heterogeneity, orographically generated waves, inertial oscillations of the nocturnal jet, and other unknown sources (Caughy and Readings 1975; Hooke et al. 1973; Thorpe and Guymer 1977; Acevedo and Fitzjarrald 2001, 2003; Blumen et al. 2001; Newsom and Banta 2003; Poulos et al. 2002; Mahrt and Vickers 2002; Soler et al. 2002; Sun et al. 2002; Van de Wiel et al. 2002a,b; Fritts et al. 2003). One-dimensional modeling of this intermittent behavior in the nighttime boundary layer has been reported by Reville (1993), and of the stably stratified case (Wyngaard 1975; Galmarini et al. 1998), but the underlying turbulent transfer mechanisms are not yet clearly understood. Recent advances in direct numerical simulation techniques have begun to show promise in the study of this problem with solutions for  $Re > 10\,000$  (Werne and Fritts 1999, 2001), as well as at lesser  $Re$  (Riley and Lelong 2000; Barnard 2000).

The nonstationarity associated with the mechanisms described above contributes to the problems encountered in attempts to model near-surface statically stable conditions, when the Brunt–Väisälä frequency  $N$  and therefore the bulk Richardson number  $Ri_b$  [see (5)], are greater

than 0 (Delage 1997). This lack of knowledge inhibits the development of reliable parameterizations of the very dynamically and statically stable nighttime boundary layer. Several efforts, for example, have attempted to identify the source(s) of errors in surface layer parameterizations for stable flows identified by Carson and Richards (1978) and Louis (1979), specifically drastic model surface cooling. It is argued by Poulos (1996) that oscillations in the stable surface layer parameterization can occasionally induce unrealistic cooling under low wind conditions. This gradient is enhanced by the turbulence parameterization and, in some cases, “runaway” cooling can occur. This nonphysical behavior is also discussed by Mahrt (1998b) to be the result of radiatively driven heat loss that is not sufficiently compensated for by the heat flux calculated in the stable surface layer parameterization. This aspect is further complicated by the important inclusion of soil variables on NBL evolution, such as soil moisture, a variable that is generally poorly initialized in numerical models (Banta and Gannon 1995); soil freezing (Viterbo et al. 1999); and soil model total heat capacity (Derbyshire 1999).

In many cases, the parameterized surface layer fluxes are inadequately matched to the formulation of the turbulent diffusion parameterization that is responsible for diffusing strong radiative cooling to greater heights. Derbyshire (1999) has recently examined this problem by a combined numerical and theoretical study ascribing the cause of numerical model failure (unrealistically large cooling) to a positive feedback. The positive feedback arises as a result of the no-slip boundary condition, where 1) near the surface, radiative cooling strengthens static stability thereby decreasing frictional retardation of flow; 2) near-surface flow accelerates, increasing shear immediately next to the surface, but reducing shear above this layer where the turbulence parameterization operates; and 3) the increased flow speed immediately next to the surface causes the surface layer sensible heat flux to increase there, causing more cooling, but higher above the reduced shear reduces the turbulent transfer of warm inversion air downward. This effect was not found by Derbyshire to require a sharp cutoff in drag at the critical Richardson number ( $Ri_c$ ) which is consistent with the pathology of model overcooling experienced by the authors. Furthermore, Derbyshire presents evidence that in fact this may be a natural occurrence that is otherwise intolerable in our necessarily imperfect numerical models of the boundary/atmosphere interface. So, to improve these parameterizations a more accurate physical basis must be found for the clear-sky NBL condition, when dynamically stable conditions ( $Ri > Ri_c$ ) often exist.

#### *b. The surface layer parameterization*

It is instructive to evaluate some of the formulations used in atmospheric numerical models to identify areas for improvement. The surface layer parameterization, in

practice, simply calculates fluxes between the location just above ground where  $U = 0$  (which defines the roughness length  $z_0$ ) and the first model grid point above ground ( $z_1$ ), effectively defining a fixed surface layer depth. The height of  $z_1$  varies depending on modeling application and user preference from typically 1 to 200 m. Thus, in a practical sense, an effective surface layer parameterization in any model will have to account for the behavior of the atmosphere between the ground and  $z_1$ , with some accounting for the influence of nonlocal sources on flux. So, quite frequently the surface layer in the model as defined by the  $z_0$  to  $z_1$  layer, is not related physically to the evolving surface layer in the atmosphere during the diurnal cycle. The problems associated with the arbitrary selection of the surface layer height in model simulation is further exacerbated by the inability to define a surface layer per similarity theory in stably stratified conditions, particularly those nocturnal conditions where winds are weak, and static stability high. With a no-slip boundary condition, shear only becomes small when weak winds are present at  $z_1$ . Above  $z_1$  in a numerical model, various forms of turbulence or boundary layer parameterization are responsible for transport of quantities.

The grid cell average surface layer kinematic eddy momentum flux can be generically defined using similarity assumptions as

$$[(\overline{u'w'})^2 + (\overline{v'w'})^2]^{1/2} = u_*^2 = a^2 \overline{U}^2 F_m\left(\frac{z}{z_0}, \text{Ri}\right), \quad (1)$$

where  $u_*$  is the friction velocity,  $a^2$  is the neutral drag coefficient,  $\overline{U}$  is the mean horizontal wind, and  $F_m$  is a stability correction to the drag coefficient for momentum dependent on  $z$ ,  $z_0$ , and  $\text{Ri}$ . As necessitated by the discretization of the Navier–Stokes equations, and in particular the use of  $\Delta z$ ,  $\text{Ri}$  is most often approximated to the surface using  $\text{Ri}_b$ , or using a substitute relationship based on Monin–Obukhov length,  $L$  (Launiainen 1995; Holtslag and Ek 1996; van den Hurk and Holtslag 1997). Analogous general formulae for heat and moisture can be written by substituting a stability-corrected drag coefficient for heat  $F_h$ , and their surface layer kinematic fluxes are then

$$\overline{w'\theta'}_0 = u_* \theta_* \quad \text{and} \quad \overline{w'q'}_0 = u_* q_*, \quad (2)$$

respectively, where  $\theta_*$  and  $q_*$  are the appropriate scaling parameters. Using the constant flux assumption (Monin and Obukhov 1954), the surface fluxes (1) and (2) are assumed to equally represent the fluxes at  $z_1$ . Temperature can be substituted for  $\theta$  with no loss of generality. Note that (1) contains no dependence on horizontal scale and is thus applied similarly for a grid cell for any grid configuration. Under nocturnal, weak wind, clear sky conditions, this formulation will mix the cooler, low-momentum air at the model surface with warmer, faster-moving air at the first model grid point above ground.

A large number of surface layer parameterization for-

mulations have been proposed, with a considerable number that have somewhat similar characteristics (many of these are described by, e.g., Yaglom 1977; Sorbjan 1989; Delage 1997; van den Hurk and Holtslag 1997; Andreas 2002). For simplicity, from this group we chose two representative parameterizations that retained characteristic behavior of a number of parameterizations currently in use, but that use  $\text{Ri}_b$  for stability correction. The specific parameterizations tested herein for statically stable conditions are those proposed by Louis et al. (1981) and Delage (1997).

Using a ratio of eddy conductivity to eddy diffusivity of one, the formulation of Louis et al. (1981; see also Kim and Mahrt 1992) can be written as

$$u_*^2 = \left[ \frac{k}{\ln\left(\frac{z}{z_0}\right)} \right]^2 \overline{U}^2 \left[ 1 + \frac{(10\text{Ri}_b)}{(1 + 5\text{Ri}_b)^{1/2}} \right]^{-1}, \quad (3)$$

$$\theta_* = \left[ \frac{k}{\ln\left(\frac{z}{z_0}\right)} \right]^2 \frac{\overline{U} \Delta \theta}{u_*} [1 + 15\text{Ri}_b(1 + 5\text{Ri}_b)^{1/2}]^{-1}, \quad (4)$$

where

$$\text{Ri}_b = (g \Delta z \Delta \theta) / \overline{U}^2 \overline{\theta} \quad (5)$$

is the bulk Richardson number, and  $k = 0.40$  is the von Kármán constant, and  $\Delta \theta$  is the temperature gradient from  $z_0$  to  $z_1$ . The quantity  $a^2 = [k/\ln(z/z_0)]^2$  is generally known as the neutral drag coefficient ( $C_{\text{DN}}$ ). Under this formulation, which is a modified form of that originally proposed by Louis (1979), the stability-corrected drag coefficient for heat reduces more slowly at high  $\text{Ri}_b$ , resulting in relatively greater surface layer heat flux. Still Louis et al. (1981) shows that it drops by over an order of magnitude as  $\text{Ri}_b \rightarrow 1.0$ , and we find it approaches zero as  $\text{Ri}_b \rightarrow 3.0$ .

The Delage (1997) formulation is also a modification to the Louis (1979) formulation, amounting to a simple increase in the value of one constant from 4.7 to 12. Though simple, Delage (1997) shows that this formulation has some of the characteristic behavior at large  $\text{Ri}_b$  of that proposed by Beljaars and Holtslag (1991), which uses  $L$  as a basis for its stability correction, and does not contain a critical  $\text{Ri}_b$  where turbulent fluxes would become zero (e.g., Holtslag and De Bruin 1988). The Delage (1997) formulation can thus be written as

$$u_*^2 = \left[ \frac{k}{\ln\left(\frac{z}{z_0}\right)} \right]^2 \overline{U}^2 [(1 + 12\text{Ri}_b)^{-1}]^2, \quad (6)$$

$$\theta_* = \left[ \frac{k}{\ln\left(\frac{z}{z_0}\right)} \right]^2 \frac{\overline{U} \Delta \theta}{u_*} [(1 + 12\text{Ri}_b)^{-1}]^2. \quad (7)$$

## 2. Data and comparison with Louis et al. (1981)

### a. Relevant field observations summary

The CASES-99 field experiment was held during the month of October 1999 over the relatively flat terrain (average slope of  $\sim 0.1^\circ$ ) of southeast Kansas (Poulos et al. 2002). During CASES-99 high-resolution information with height was obtained by a 60-m tower outfitted with an unusually dense vertical array of fast-response sensors. The instruments relevant to the current study include six levels of either Campbell Scientific CSAT3 or Applied Technologies K-style sonic anemometers (at 0.5 or 1.5, 5, 10, 20, 30, 40, 50, and 55 m, respectively) sampled at 20 samples per second (sps), 34 levels of E-type fine-wire thermocouples (from 0.23–58.1 m) sampled at 5 sps, four levels of RM Young Model 9101 Prop/Vane Anemometers (at 15, 25, 35, and 45 m), and six levels of slow-response aspirated temperature/humidity sensors (at 5, 15, 25, 35, 45, and 55 m). Poulos et al. (2002) has more detailed information about the CASES-99 60-m tower instrumentation.

The thermocouple temperature data were processed based on the six slow-response sensors. Based on comparisons with the aspirated temperature data, the nighttime thermocouple temperature has an absolute accuracy of about  $0.15^\circ\text{C}$ . The mean wind and turbulent flux data used for the analysis herein are from the 5-min-averaged data from the National Center for Atmospheric Research (NCAR) Atmospheric Technology Division (ATD). Covariances are computed over a 5-min period, which should be short enough to exclude most mesoscale influences on the fluxes, but long enough to capture most of the turbulent flux, during statically stable conditions (Howell and Mahrt 1997). To minimize flow distortion effects on the sonic anemometer measurements, all data with a wind direction between  $250^\circ$  and  $290^\circ$  were neglected in this study (the sonic anemometer booms pointed to the east). The 5-Hz thermocouple data were averaged over the same 5-min periods.

### b. Data analysis

The data were used to calculate  $Ri_b$  from (5) between each level and the ground in 5-min intervals for a 10-h period during the nighttime, 0000–1000 UTC (1900–0500 LST). By calculating  $Ri_b$  between the ground and a sonic anemometer level, we mimic the calculations made by a numerical model between  $z_0$  and  $z_1$ . To calculate  $Ri_b$ , the surface temperature was estimated using the mean temperature measured by five downward-looking narrow-beam Everest Interscience infrared radiometers, which were within 300 m of the 60-m tower. The vertical gradient of wind was determined by combining the sonic and prop/vane wind speed data at the appropriate level and using zero wind speed at  $z_0$  by definition. For comparison purposes, a second estimate of the surface temperature was made with the 0.23-m

thermocouple (near the top of the vegetation). During nighttime, the 0.23-m thermocouple and five-station-averaged radiative temperature were typically within about  $1^\circ\text{C}$ . This difference was slightly larger for low wind speed conditions. Examples of  $Ri_b$  calculated using the 0.23-m thermocouple and five-station-averaged radiative temperature are shown in Fig. 1a. With knowledge of  $Ri_b$ , and assuming  $z_0 = 0.01$  (typical of plains grassland), (3)–(7) can then be used to calculate  $u_*$  and  $\theta_*$ . These parameters are then combined to create sensible heat flux ( $H_p$ ) for comparison to the eddy-correlation sensible heat fluxes ( $H$ ) measured by the sonic anemometers, and  $u_*$  is compared directly with the calculations of  $u_*$  from the sonic anemometers. We choose herein to focus on the behavior of the Louis et al. (1981) and Delage (1997) formulas for  $u_*$  and  $\overline{w'\theta'}$  (or equivalently,  $u_*\theta_*$ ) at large  $Ri_b$ . To what degree might the parameterization be in error, for a large range of  $Ri_b > 0$ , compared with measured  $u_*$  and  $H$ ?

The various sonic levels are taken to represent, in effect, potential user-defined vertical grid configurations or  $z_1$ . In current modeling applications,  $z_1$  is generally selected based on numerical considerations and computational efficiency, without much concern for the physics of the NBL, the surface layer, or the assumptions in surface layer theory. Given the relative shallowness of the surface layer underlying the NBL compared to that in the convective boundary layer, this approach is perhaps as satisfactory as any. Further, given the inadequacy of surface flux measurements using sonic anemometers when the measurement height falls below  $\sim 5$  m (Mahrt 1998a; Howell and Sun 1997) and the sampling frequency is low, the relative importance of this selection is probably low. That said, we should hope that our modified similarity theory-based surface layer schema, such as those tested herein, satisfactorily approximate the behavior of the real NBL, regardless of  $Ri_b$ .

For brevity, we have chosen to present results based primarily on measurements taken at 20 m, with lesser discussion of results derived from the 10-m and 50-m heights, although a variety of tests were made for the other sonic levels to ensure the adequacy of our conclusions. Furthermore, we have limited our investigation to those cases where  $Ri_b > 0$ , with a particular focus on the very stable case where fluxes generated by intermittent turbulence can dominate transport. Theoretical and observational studies indicate that the critical  $Ri$  for the onset of turbulence is met when  $Ri < \sim 0.25$  (Ellison 1957; Woods 1969; Stewart 1969; Oke 1970; Arya 1972; Yamada 1975). Since our  $Ri_b$  are calculated using the bulk formula, this limit is not strictly applicable, less so as  $\Delta z$  increases. When  $Ri$  exceeds 1.0, buoyant suppression of turbulence overcomes the shear production, and thus momentum and scalar fluxes become negligible [although radiative flux divergence is likely to be significant (Funk 1960)], in the absence of external sources.

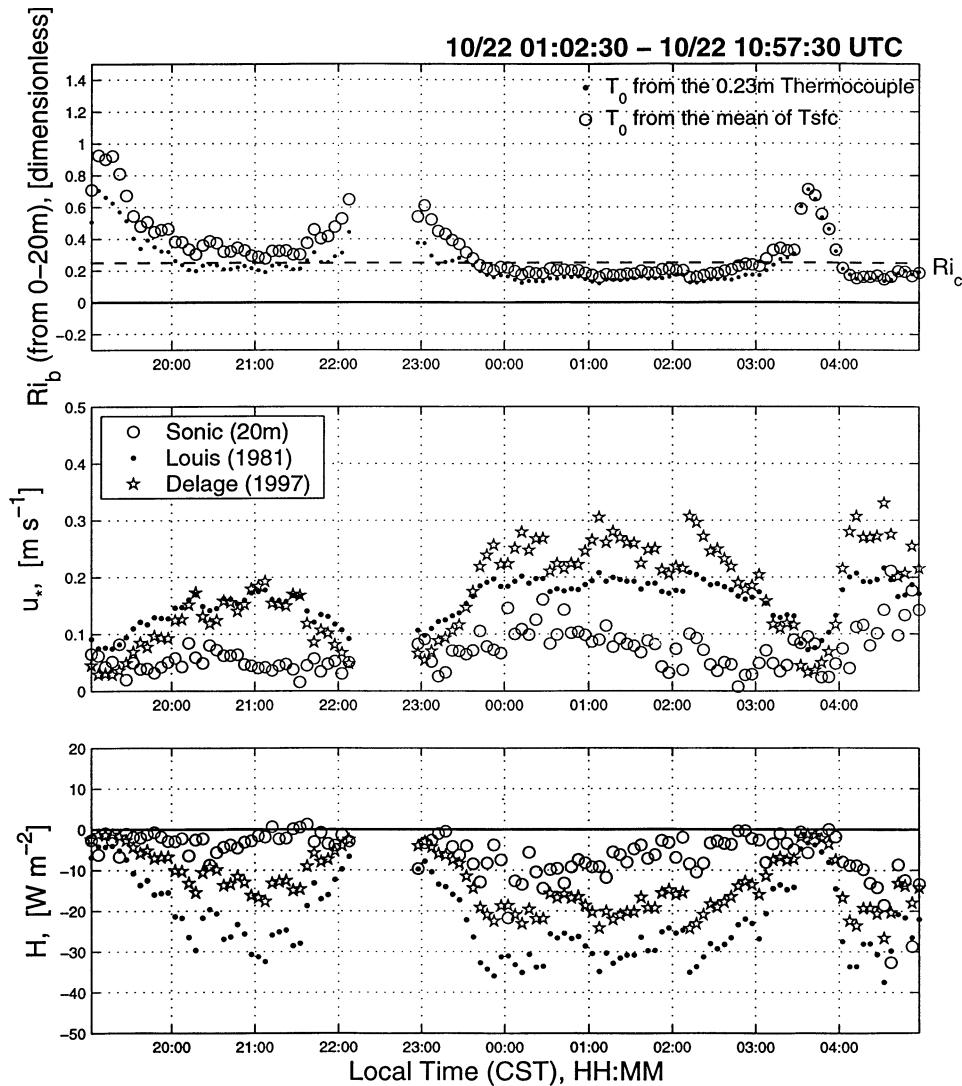


FIG. 1. A sample time series 1900–0500 LST 22–23 Oct 1999 from CASES-99: (a)  $Ri_b$  calculated using a temperature gradient between 20 m and the surface vs time. The surface temperature was evaluated in two ways: 1) with the mean infrared temperature of five sensors within 300 m of the 55-m tower (open circles) and 2) using the thermocouple temperature at the height (0.23 m) of the local grasses (dots). (b) As measured at 20 m  $u_*$  vs time (open circles) and calculated from the Louis et al. (1981) formulation (dots) and the Delage (1997) formulation (stars). (c) As measured at 20 m  $H$  vs time (open circles) and calculated from the Louis et al. (1981) formulation (dots) and the Delage (1997) formulation (stars).

### c. The evolution of $u_*$ and $H$ with changes in $Ri_b$

Since we seek to refine the relationship between surface layer fluxes and  $Ri_b$ , it is useful to review the behavior of observed  $u_*$  and  $H$  with evolving overnight  $Ri_b$ , to determine whether any unexpected relationships may be present. In our investigation of time series such as Fig. 1 for all CASES-99 nights, we find no clearly dominant pattern of behavior. At times, we find the theoretical expectation that as  $Ri_b$  decreases, turbulence increases, and vice versa. At other times, no relationship or an inverse relationship exists. Of course, this inconsistent behavior can be explained by the use of  $Ri_b$  rather than  $Ri$ , so that the local measurement by the sonic

anemometer at a given height is not representative of  $Ri_b$ , which is calculated from the ground to 20 m. However, these are precisely the conditions under which surface layer formulations such as (3) and (4) are expected to perform well in reproducing the behavior of the near-surface atmosphere.

An example of the behavior of  $u_*$ ,  $H$ , and  $Ri_b$  is shown in Fig. 1 for one of the 10-h periods from overnight on 22–23 October for a height of 20 m on the 60-m tower. Let us follow the time progression of  $Ri_b$  as calculated using skin temperature in Fig. 1a and observed  $u_*$  and  $H$  (all indicated with open circles). First, we note that the decrease of  $Ri_b$  from 1900 LST from 1.0 to  $\sim 0.20$

( $Ri_b$  of  $\sim 0.20$  lasts then for about 2 h) is not accompanied by a significant increase in either observed  $u_*$  or  $H$  (Figs. 1b and 1c, respectively). As mentioned previously, if these measurements were of  $Ri$  rather than  $Ri_b$ , we would expect a decrease in  $Ri$  to correspond with an increase in turbulent fluxes, but in this case we show that  $Ri_b$  is not so correlated. After 2200 LST, we see that the values of  $Ri_b$  increase again to about 0.6, before and after a period of missing data. This period of generally greater  $Ri_b$  is not associated with lower  $u_*$  and  $H$ , as would be expected, but rather similar or slightly larger  $u_*$  and magnitude of  $H$ . Starting about 0000 LST,  $Ri_b$  again is  $\sim 0.2$  for a period of 3 h. Although  $u_*$  and  $H$  are somewhat larger in magnitude (they actually gradually decrease in magnitude through the 3-h period) than during the previous lower  $Ri_b$  period, they are not so different than the high  $Ri_b$  period preceding them. Between 0325 and 0355 LST,  $Ri_b$  again increases significantly to a peak value of nearly 0.8. Compared to the immediately preceding period of lower  $Ri_b$ , there is not a notable response in the observed value of  $u_*$  or  $H$ , although the values are lesser in magnitude than the average values for the entire 3-h period. Finally, at the far right-hand side of the plot, we note that  $Ri_b$  drops to  $\sim 0.2$  for a period of 1 h. In this case, more traditional behavior prevails in the observations; both  $u_*$  and  $H$  increase significantly in magnitude, suggesting an increase in turbulent mixing.

Although the behavior of the observed fluxes does not necessarily follow the theoretical relationship between  $Ri$  and fluxes at all times, the Louis et al. (1981) and Delage (1997) formulas must. Inspecting the low  $Ri_b$  periods we find a general overprediction of both heat and momentum flux. At higher  $Ri_b$ , the Louis formula shows somewhat larger magnitude  $u_*$  values, while the Delage-based values are relatively smaller in magnitude, though it is not possible to describe the adequacy of their performance from this plot alone. The implications of these observations is very significant as described further below. All of the above descriptions are valid for  $Ri_b$  calculated using thermocouple temperatures located at the top of the local roughness elements (see black dots in Fig. 1a). We found that the thermocouple temperatures were generally 1 K warmer than the average skin temperature, resulting in slightly lower overall  $Ri_b$  values per (5).

### 3. Analysis

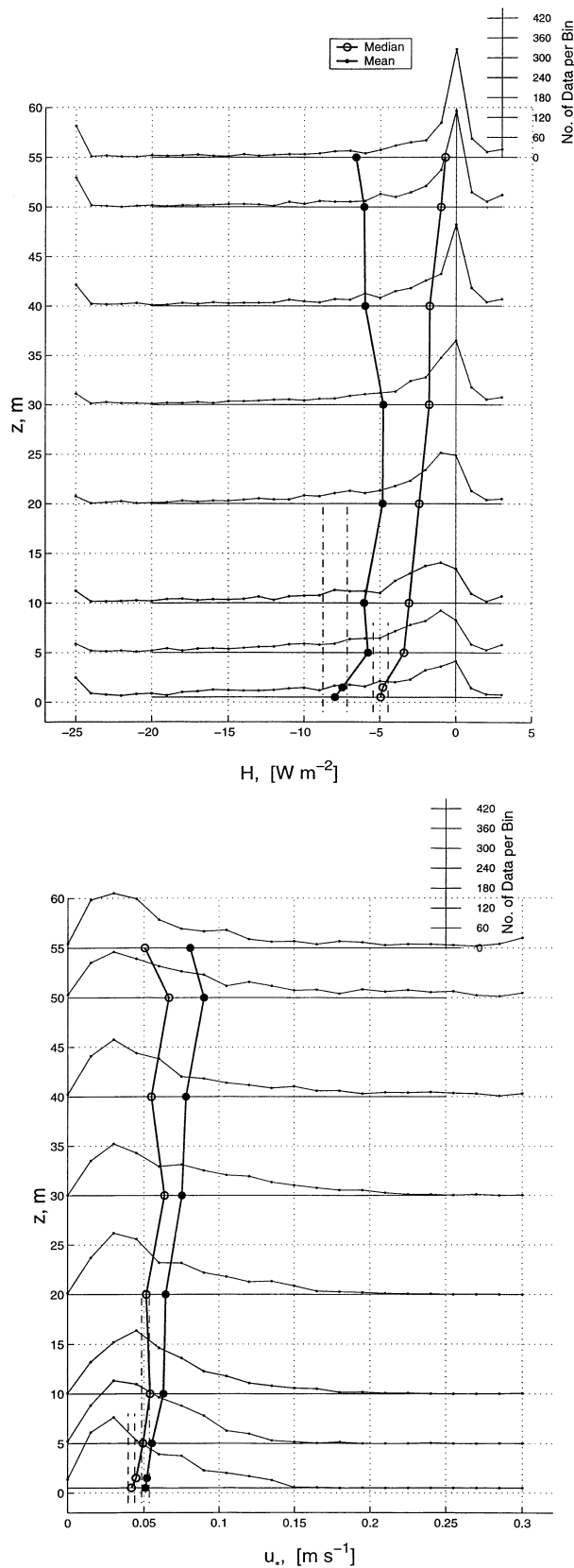
#### a. The constant flux assumption

Given the use of the constant flux assumption in the application of the Louis et al. (1981) and Delage (1997) formulas and the known problems with their application for high  $Ri_b$ , it is of interest to use the experimental data to evaluate flux profiles (e.g., Elliott 1964), estimate the depth of the surface layer, and assess the validity of the constant flux assumption for positive  $Ri_b$ . The depth

of the surface layer is defined as that height where the given flux changes by a some mathematically tolerable threshold fraction of its maximum value near the surface (Monin and Obukhov 1954). Generally, fluxes are expected to decrease in magnitude with height from the surface, and nearly linearly for a uniform lower boundary. A commonly used value for this threshold is 10%, although Monin and Obukhov (1954) used 20% for that depth through which momentum flux is “practically” constant in neutral conditions (see also Obukhov 2001, p. 164). As stated by Panofsky and Dutton (1984), there is no precise quantitative definition of the surface layer, and for  $u_*$ , a threshold of 5% is appropriate. For this analysis we have chosen to stratify the data based on  $Ri_b$ , as calculated from the 20-m level. Also, since the 1.5-m sonic anemometer was lowered to 0.5 m halfway through the experiment, these data were linearly interpolated or extrapolated to create a continuous time series at both 0.5 and 1.5 m for the generation of flux profiles.

Figure 2 presents the mean and median profiles of  $H$  and  $u_*$  with height for all  $Ri_b > 0.2$ . Distributions of all  $H$  are shown for each sonic anemometer height available (Fig. 2a), where the data have been binned to create the distributions and all data above  $+3 \text{ W m}^{-2}$  are summed in the final bin on the right-hand side, while all data below  $-25 \text{ W m}^{-2}$  is summed in the final bin on the left-hand side. The distributions indicate that the number of extreme events increases with altitude above ground, particularly in the case of strong negative heat flux events. In response to those large events, the mean  $H$  profile is not monotonic; as height increases above 20 m, the mean value moves toward larger negative values. This tendency is consistent with Mahrt’s (1999) notion of an “upside-down boundary” layer. The median profile does not respond to extreme events by definition, and decreases monotonically toward zero. In all cases, the distribution is skewed negative and non-Gaussian, although closer to the surface roughness elements the tendency for fewer extreme and zero events is evident.

We note that the depth of the traditional surface layer (where the vertical dashed lines intersect the mean and median profiles of  $H$ ) in this case is approximately 2 m using a 10% threshold. Note, however, that actual magnitude of the mean  $H$  profile does not change much with height and is not monotonic, making the estimate difficult to interpret (or even defining a boundary layer difficult). Indeed, similar plots limiting the data to higher and higher  $Ri_b$  indicate that the surface layer becomes less well defined with increasing bulk stability (in part due to decreasing numbers of available data). As has been discussed by Mahrt (1999) the NBL is difficult to define as static stability increases, so we would expect the surface layer to be likewise difficult to evaluate. A plausible physical interpretation of this mean profile is suggested by the frequency of low-level jets of 7–10  $\text{m s}^{-1}$  at  $\sim 100 \text{ m AGL}$  observed during CASES-99 (Poulos et al. 2002; Banta et al. 2002). The first 20 m AGL,



in which the heat flux decreases with height, represents a portion of a traditional surface-based nocturnal boundary layer (which is also consistent with a 2-m-deep surface layer). The region from 20–55 m AGL, where the heat fluxes again increase, is sensibly considered a consequence of shear-generated turbulence beneath the low-level jet that results in downward transport of heat from the inversion aloft. In combination, rather than an upside-down boundary layer, in the mean for heat flux we find “mirrored” boundary layers.

The equivalent plot for  $u_*$  is shown in Fig. 2b. Here we find mean and median profiles that are even less amenable to interpretation relative to the surface layer than the  $H$  profiles. Rather than decreasing with height toward zero,  $u_*$  increases with height. In this case, the source of momentum flux is aloft, consistent with low-level jet formation and weak near-surface winds, and a traditional surface layer is not present (though we have drawn lines indicating the 10% threshold for consistency). This profile more favorably compares with the concept of the upside-down boundary layer (Mahrt and Vickers 2002), but contrasts the mirrored profile of mean  $H$ . Mean vertical profiles of temperature (not shown) indicate that the strongest potential temperature increases occur on average below 10 m AGL and in the inversion aloft, with much smaller temperature gradients between these regions. Combined with mean profiles that show increasing wind speed with height, we can logically conclude that in the mean, where large-magnitude intermittent heat flux events contribute to the profile shape, the mirrored heat flux profile would exist.

The implications of the inability to define a traditional boundary layer, and also a surface layer, is significant for numerical modelers (please reference section 1b). Since  $z_1$  defines the numerical model’s surface layer height, according to Fig. 2, it should be placed at a few meters if proper representation of overnight surface heat fluxes over approximately flat terrain is desirable. Placing such a constraint on numerical model configuration creates significant computational challenges. However, if we consider that other assumptions (e.g., continuous turbulence) of similarity theory are also violated in the dynamically stable regime, and that during daytime such a selection for  $z_1$  would be too small, the relative benefits of strict adherence to the constant flux assumption is perhaps limited. Nevertheless, we would expect failure of surface layer schemes on the basis of this information, for higher  $Ri$  or  $Ri_b$  even if constrained by observational data.

FIG. 2. (a) Mean and median  $H$  vs height for all valid CASES-99 data between 1900 and 0500 LST, overlaid on the distributions of  $H$  at each height for all data where  $Ri_b$  at 20 m was greater than 0.2. (b) As in (a) but for  $u_*$ . The depth of the theoretical surface layer is shown by where the vertical dashed lines intercept the mean and median profiles.

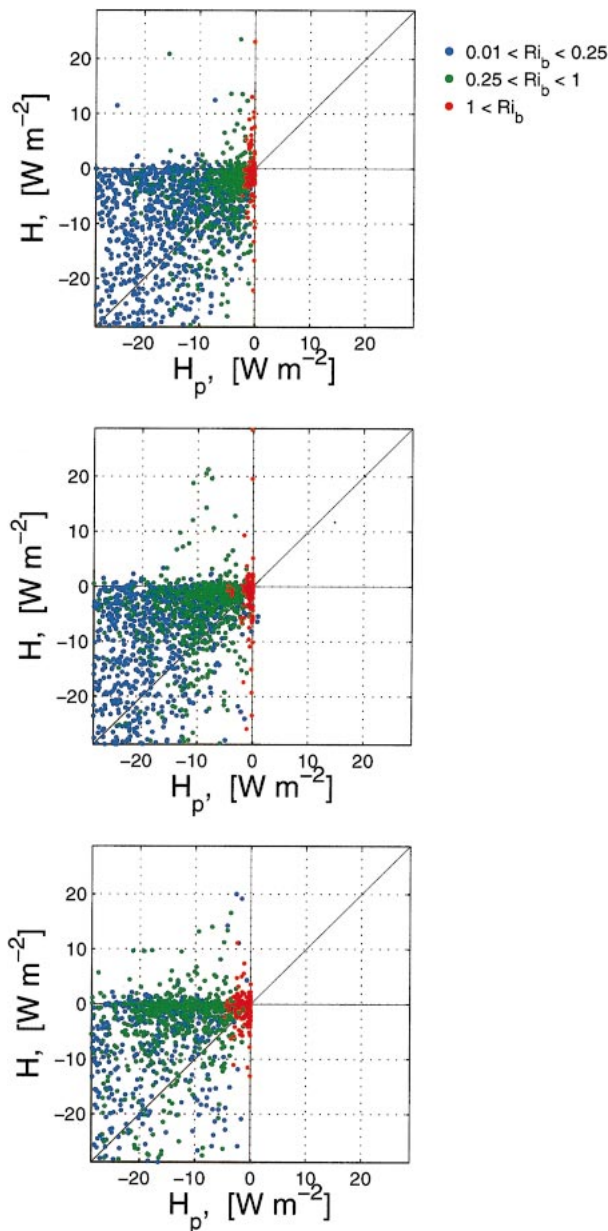


FIG. 3. From the Louis et al. (1981) formulas  $H$  vs  $H_p$  for heights of (a) 10, (b) 20, and (c) 50 m for  $Ri_b > 0.01$ .  $0.01 < Ri_b < 0.25$  (in blue),  $0.25 < Ri_b < 1.0$  (in green), and  $1.0 < Ri_b$  (in red).

## b. Formulation evaluation

### 1) $H$ VERSUS $H_p$

Figure 3 compares the heat fluxes measured by the sonic anemometer  $H$  versus the Louis et al. (1981) parameterization heat flux  $H_p$  at three levels and reveals some inadequacies. First, all  $H_p$  are negative, whereas a significant fraction of the actual sensible heat fluxes are greater than zero (tabulated further below);  $H > 0$  indicates potential flux contamination by wave activity (Chimonas 1985) but also corresponds to external and

vertically localized flux sources, such as density currents. Second, even when  $H$  is negative,  $H_p$  is systematically too small at  $Ri_b > 1.0$  (red dots), as also shown in Table 1 comparing column 6 to column 8. Although the Louis et al. (1981) formula has been modified to maintain fluxes to larger  $Ri_b$  than the Louis (1979) scheme, it continues to significantly underestimate them, even for this relatively simple field experiment location. For  $Ri_b > 1.0$  (up to as high as  $Ri_b \sim 30$ ), this underprediction is so severe that all errors approach 100%.

The latter observation is consistent with an underestimated transfer of cold surface (radiationally cooled) air upward when  $Ri_b > 1.0$ , compared with the atmospheric behavior measured during CASES-99. Thus, the erroneously low surface temperatures occasionally found in numerical models may be caused by this underprediction, assuming this conclusion is globally applicable. If  $H_p$  is systematically too small at high  $Ri_b$ , then for that case, the other components must compensate in the surface energy balance. It has been shown by Derbyshire (1999) and Viterbo et al. (1999) that due to the large thermal inertia of soil relative to the air, the soil heat flux term can be a dominant source of adjustment. The latent heat flux, which is also parameterized with similar relationships to (1), could also be underestimated (not to mention subject to the well-known errors in soil moisture representation, and contributions from the complexities of vegetation parameterization). Thus, the radiative term (calculated by the radiative parameterization) is the only other surface energy balance component that can compensate for the potentially non-physical evolution of near-surface temperature via radiative flux divergence.

In theory, the radiation should be able to accomplish this balancing, but in practice, it cannot. First, radiative schemes are expensive and radiative tendencies are thus frequently calculated at a rate considerably slower than a typical numerical model time step. For example, in the Regional Atmospheric Modeling System (RAMS; Pielke et al. 1992), it is a frequent practice to use time steps near 30 s and run the radiation scheme every 600–1200 s. Thus, the radiative scheme cannot adjust to time step-to-time step excess cooling being generated by  $H_p$  at  $z_1$  when  $Ri_b > \sim 1.0$  in overnight conditions. To a lesser degree, the fact that most radiation schemes are considerably simplified versions of the full radiative transfer equations (e.g., 1D and limited in spectral content), can be a factor. Given the complex orography in much of the land-covered portion of the earth, the lack of a horizontal radiative component can become significant where grid spacing is small enough to resolve steep terrain. As is commonly found in basins, orography can also make such parameterization problems more evident, as light winds and statically stable layers are more frequent. One can rationally suggest that to partially counteract the tendency for bias toward low temperatures, modelers can more frequently run their

TABLE 1. For all points where  $Ri_b$  falls within certain bounds at 10, 20, and 50 m, the number of points in the category, and the  $Ri_b$ ,  $H$ ,  $H_p - H$ , and  $H > 0$  statistics;  $H_p$  values are for the Louis et al. (1981) formulation only.

Tower level (m AGL)	$Ri_b$ range	No. of points	$\overline{Ri_b}$	$Ri_b$ median	$\overline{H}$ ( $W m^{-2}$ )	$H$ median ( $W m^{-2}$ )	$\overline{H_p - H}$ ( $W m^{-2}$ )	$H_p - H$ median ( $W m^{-2}$ )	$H_p - H$ $\sigma$ ( $W m^{-2}$ )	% of $H > 0$
10	0.01–0.25	1591	0.09	0.08	−18.27	−12.04	−0.13	−1.62	15.5	2.8
20	“	1577	0.10	0.09	−21.34	−14.29	0.15	−3.38	17.9	2.8
50	“	1338	0.12	0.11	−28.81	−24.68	0.74	−1.90	24.0	4.2
10	0.25–1.0	432	0.47	0.41	−2.40	−1.74	−1.38	−1.60	4.3	16.4
20	“	587	0.44	0.37	−2.44	−1.44	−4.85	−4.27	5.3	14.8
50	“	741	0.42	0.38	−2.24	−0.60	−11.16	−10.72	8.8	26.2
10	1.0–4.0	97	1.83	1.54	−0.66	−0.36	0.16	−0.09	3.1	36.1
20	“	142	2.03	1.80	−1.13	−0.47	0.50	−0.17	2.4	27.5
50	“	201	1.99	1.82	−0.49	−0.15	−0.71	−0.67	1.9	33.8
10	>4.0	32	18.35	6.30	−0.69	−0.41	0.65	0.37	2.3	31.2
20	“	39	11.81	7.45	−1.49	−0.63	1.45	0.61	3.1	33.3
50	“	81	10.27	7.67	−0.46	−0.12	0.38	0.05	1.2	42.0

radiative schemes, allowing for a smoother and perhaps stronger adjustment to inadequacies of the surface layer scheme at high  $Ri_b$ .

Figure 3 also shows some intersecting trends in behavior with increasing  $Ri_b$ . At relatively low, but positive  $Ri_b$  (blue dots) a greater fraction of  $H_p$  are too high at all three levels, but the range of  $H$  and  $H_p$  is similar. At 10 m, the overprediction is somewhat less than that at 20 or 50 m. This trend can be attributed to more continuous down gradient transfer near the surface where external influences are less dominant. A similar trend of overprediction is found for  $0.25 < Ri_b < 1.0$ , but also the range of  $H_p$  becomes much larger with height, while the range of observed sensible heat flux narrows. For  $Ri_b > 1.0$ , the tendency for  $H_p$  to approach zero mutes this trend, but at 50 m the range of  $H_p$  is greater than at lower levels. The range of  $H$  for  $Ri_b > 1.0$  does not appear to change, unlike at lower  $Ri_b$ . One can conclude from these observations that the performance of the Louis et al. (1981) scheme is dependent on height above ground in some manner that is not captured by the  $z/z_0$  dependency in (3) and (4).

Table 1 also shows some interesting trends in behavior relevant to the representation of the surface layer numerical models. First, we note that the number of data points available for a given  $Ri_b$  threshold diminishes by approximately 150 times for a given height per the first three columns. The numbers are reasonably high, however, even for  $Ri_b > 4.0$ , particularly considering these are 5-min averages. The difference between the relatively higher mean and the median  $Ri_b$  values emphasizes the scatter of the data and also the sensitivity of the mean to outliers (see especially  $Ri_b > 4.0$ ). This point is reinforced by the mean and median  $H$  values, in columns 6 and 7, indicating a broad range of  $H$  for a given  $Ri_b$  threshold. Those same columns show that with increasing  $z$ , the scatter increases for  $0.25 < Ri_b < 1.0$ ; the mean  $H$  stays approximately constant with height (or layer thickness), while the median decreases

in magnitude, because the median is not sensitive to strong intermittent turbulent events (recall from Fig. 2 that more extreme flux events occur at greater heights than at lower heights). This trend disappears for  $1.0 < Ri_b < 4.0$  and  $Ri_b > 4.0$ , and the maximum mean and median values of  $H$  shift to the 20-m-thick layer. Given the relatively high frequency of nocturnal low-level jets over the CASES-99 site, we believe the behavior of  $H$  with height for  $0.25 < Ri_b < 1.0$  can be ascribed to more widely varying wind speed at 50 m, compared with lower levels. The higher mean  $H$  at lower levels also is sensibly described as the result of stronger near-surface stratification subject to more or less continuous turbulence when any wind is present. For higher  $Ri_b$ , the maximum in  $H$  is at 20 m, although generally the values are quite small and the behavior may be physically related to the intermittent phenomena observed during CASES-99. In fact, it is important to note that mean  $H$  drops by nearly an order of magnitude for all  $Ri_b > 0.25$  thresholds, validating roughly the drag coefficient behavior in the Louis et al. (1981) scheme noted earlier. On the contrary, for  $Ri_b > 1.0$ , the mean  $H$  drops again by a factor of 2 but does not become  $\sim 0$  like Louis et al. (1981) at high  $Ri_b$ .

Columns 8–10 of Table 1 show the statistics of the parameterization error relative to observed for the different  $Ri_b$  thresholds and layer depths. Relatively little bias is indicated compared to the mean and median  $H$  for  $0.01 < Ri_b < 0.25$ , although this performance becomes somewhat worse with height. This fact emphasizes that even for lower  $Ri_b$  conditions, a relatively lower placement of  $z_1$  is warranted in numerical models. Because  $H$  reduces significantly for all thresholds where  $Ri_b > 0.25$ , but the bias (or mean  $H_p - H$ ) does not drop proportionally, the relative importance of the errors is magnified. The standard deviation of the errors, in column 10, is presented to further emphasize the increasing scatter in the data relative to the mean and median error with increasing  $Ri_b$ . The magnitude of

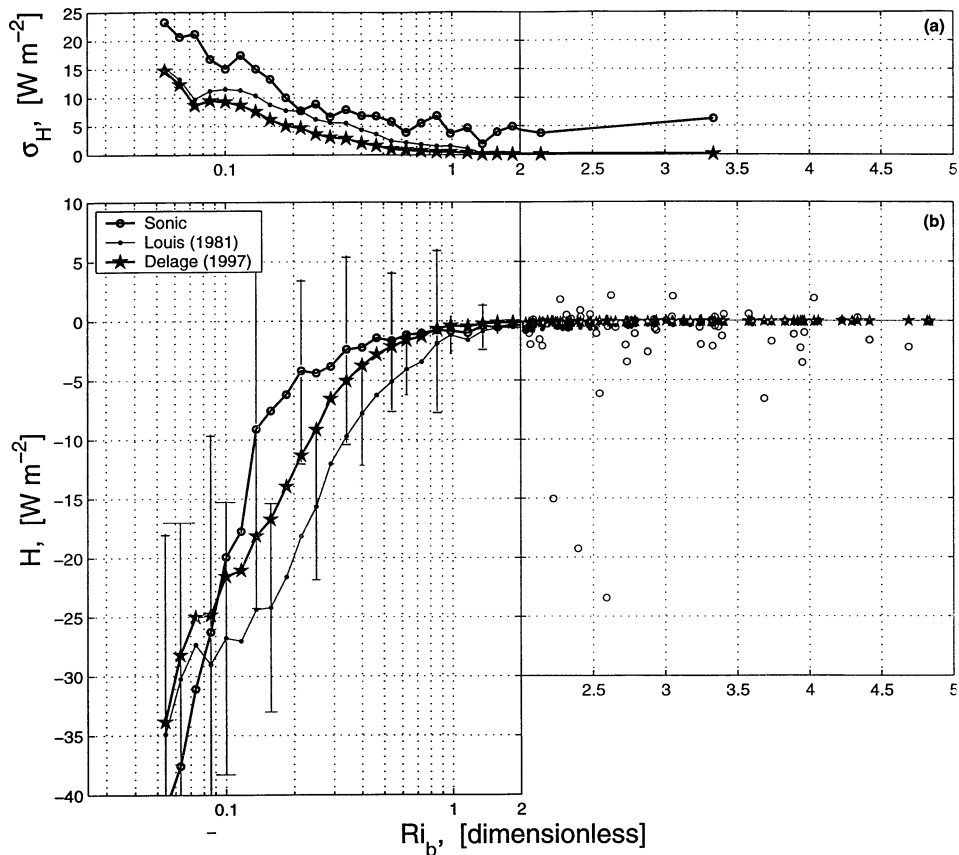


FIG. 4. (a) Here  $\sigma_H$  and  $\sigma_{H_p}$  [Louis et al. 1981 (dots) and Delage 1997 (stars)] vs  $Ri_b$ , and (b)  $H$  and  $H_p$  (Louis et al. 1981; Delage 1997) vs  $Ri_b$ . Insufficient data do not allow the drawing of a meaningful line beyond  $Ri_b = 2.0$  in (b). Std dev ranges are also shown in (b) for some of the data.

negative sensible heat flux is predicted to be considerably too high for  $0.25 < Ri_b < 1.0$ , in contrast to behavior at  $Ri_b$  outside this range. Larger magnitude negative fluxes are also found at the 50-m level for  $1.0 < Ri_b < 4.0$ , validating our observation of different behaviors at different altitudes in Fig. 3. At higher  $Ri_b$  thresholds we also note the trend of the bias (column 8) approaching the mean value of  $H$  (column 6). This is a clear indication of the questionable performance is replicating the observed  $H$  by the Louis et al. (1981) scheme. At lower levels, for example, the 10-m layer, the performance is marginally better for a given  $Ri_b$  threshold. As the  $Ri_b$  threshold increases, however, the failure of the scheme for this experiment is clear:  $H_p - H \sim \bar{H} \sim H_{\text{Median}}$ . We conclude that the Louis et al. (1981) scheme provides insufficient (nearly zero)  $H_p$  relative to observations that show a small but continued source of upward transfer of cold air, even at high  $Ri_b$ .

These conclusions are emphasized by plotting the behavior of  $H_p$  and  $H$  and their standard deviations versus  $Ri_b$  as shown in Fig. 4. In addition to the values for the Louis et al. (1981) formulation, we also include those based on Delage (1997). At other heights, a similar result is found, and thus they are not shown here. We find

that the behavior of the CASES-99 observations clearly deviates from the parameterized high  $Ri_b$  behavior of Louis et al. (1981; lines are fit to the mean of  $H$  and  $H_p$  up to  $Ri_b = 2.0$ , in Fig. 4b) and also Delage (1997). An overprediction of negative heat flux by the Louis et al. (1981) formula in the range  $0.1 < Ri_b < 1.0$  is evident (note, too, that there is no sharp transition in  $H$  at  $Ri_b \sim Ri_c$ ). Some of these average errors are quite significant. For example, at  $Ri_b = 0.2$ , the average  $H$  from CASES-99 observations is  $-4.5 W m^{-2}$ , where as  $H_p$  for Louis et al. (1981) is  $-20.5 W m^{-2}$ , nearly a four-fold increase in magnitude. Then from  $\sim 1.0 < Ri_b < \sim 2.0$  the behavior of Louis et al. (1981) improves as the lines converge, although the  $\sigma_{H_p}$  is considerably reduced from that of the observations.

The Delage (1997) formulations, (5) and (6), are shown using a star symbol in Fig. 4, and also show similar behavior as the Louis et al. (1981) formulation, although the errors are smaller at low, positive  $Ri_b$ . Specifically, overprediction of the magnitude of  $H$  is found for the range  $0.1 < Ri_b < 0.6$  and an improved mean performance is found from  $\sim 0.7 < Ri_b < \sim 1.0$ . The overprediction of  $H$  by the Delage (1997) formula for  $Ri_b = 0.2$  is approximately half that of the Louis et al.

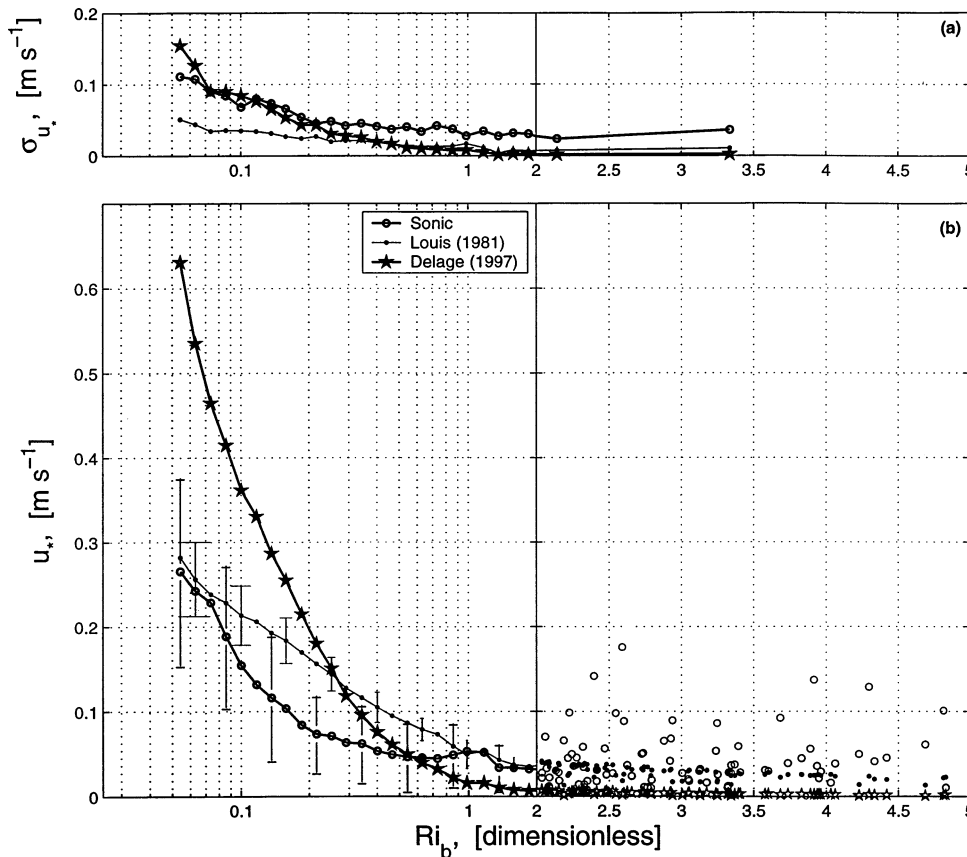


FIG. 5. (a) Parameters  $\sigma_{u_*}$  and  $\sigma_{u_{*p}}$  [Louis et al. 1981 (dots) and Delage 1997 (stars)] vs  $Ri_b$ , and (b)  $u_*$  and  $u_{*p}$  (Louis et al. 1981; Delage 1997) vs  $Ri_b$ . Insufficient data do not allow the drawing of a meaningful line beyond  $Ri_b = 2.0$  in (b). Std dev ranges are also shown in (b) for some of the data.

(1981) scheme. For  $Ri_b > \sim 1.0$  it is shown in Fig. 4 that for the Delage (1997) scheme  $H_p \rightarrow 0$  more quickly and somewhat more in error than the Louis et al. (1981) formulation (this is clearer in a plot using a reduced scale on the y axis, not shown). However, similar to the Louis et al. (1981) formulation, the standard deviation of  $H_p$  is significantly underrepresented relative to the observations.

The open circles in Fig. 4, representing  $H$  for  $Ri_b > 2.0$ , indicate that significant fluxes, as typically generated by intermittent events at high  $Ri$  continue to modify the temperature structure of the NBL. In contrast, for high  $Ri_b$  the  $H_p$  for both Louis et al. (1981) and Delage (1997) has systematically become nil. Note that there are a number of occasions at large  $Ri_b$  where  $H > 0$ , and that the fraction of occurrences increases both with increasing  $Ri_b$  (column 11 of Table 1). On the basis of mean  $H$  in the table for  $Ri_b > 4.0$  these errors translate into an unaccounted for natural heat transfer of  $3^\circ\text{C h}^{-1}$ . Although statistically significant standard deviations cannot be reliably calculated due to the small volume of data for  $Ri_b > 2.0$ , it is clear that external sources generate far larger variability in  $H$  than  $H_p$ . A significant fraction of these fluxes are large negative values and

some are moderate and positive. Using this observation, if one wished to replicate the average behavior for  $Ri_b > 2.0$ , a simple functional form as proposed by Kondo et al. (1978), where the modified drag approaches a constant minimum value is suggested. In fact, the Louis et al. (1981) scheme continues to provide very small values, and the Delage (1997) scheme even smaller values, for high  $Ri_b$  since they contain no  $Ri_c$  in their formulations.

2)  $u_*$  VERSUS  $u_{*p}$

Additional information can be gleaned regarding the physical realism of the Louis et al. (1981) and Delage (1997) formulas by observing their ability to predict  $u_*$ . In addition to defining the surface layer momentum flux,  $u_*$  is an important component in the prediction of  $H$  per (2) and the calculation of surface layer scaling parameters for heat and moisture flux. Figure 5 shows this relationship as in Fig. 4, but for  $u_*$ . Here, we find an overprediction of  $u_*$  compared with observations using (6) for all  $0.03 < Ri_b < 0.50$  (with very large errors as  $Ri_b$  approaches zero), a crossover point at  $\sim Ri_b = 0.54$ , and an underprediction of mean  $Ri_b$  for  $Ri_b > 0.54$ .

Note that  $u_*$  values are just slightly above zero for  $Ri_b > 2.0$ . The prediction of  $u_*$  by (3) is considerably more realistic for the entire  $Ri_b$  range. First, the performance at the lowest  $Ri_b$  values plotted is quite good, although for  $0.1 < Ri_b < 0.7$  there is an obvious overprediction in mean  $u_*$ . Using (2) we thus find that errors in  $u_*$  contribute toward poor performance of the Louis et al. (1981) scheme for  $H$  described earlier. For  $0.9 < Ri_b < 2.0$  the mean performance of (3) is very good, although the standard deviation of the values of  $u_*$  is quite small compared to the observations (Fig. 5a). For  $Ri_b > 2.0$ , the Louis et al. (1981) formulation maintains a significant  $u_*$  compared to Delage (1997), which is more consistent with the observations, although with far less variability as shown in Fig. 5a. These comparisons indicate clearly that the Delage (1997) formulation for small, positive  $Ri_b$  has an offsetting behavior in  $u_*$  and  $\theta_*$ , leading to a somewhat more satisfactory performance for heat flux while exhibiting great errors in momentum flux. At larger, positive  $Ri_b$ , the Delage (1997) formula's underprediction of  $u_*$  is a component of the problem in the underprediction of  $H$ . The Louis et al. (1981) scheme, on the other hand, shows considerably more accurate mean behavior for all positive  $Ri_b$  for  $u_*$ , in contrast to the prediction of  $H$ . For large  $Ri_b$  the significant  $u_*$  predicted by the Louis (1979) formula allows for somewhat more significant, though still small, values of  $H_p$  per Fig. 4. In the case of either scheme, the overall variability in momentum flux compared to its natural variability is greatly underpredicted, even for these data that are based on 5-min averages.

### 3) A DIFFERENT APPROACH

A more physically based approach to the formulation of high  $Ri_b$  parameterization schemes is suggested by the obvious divergence of parameterization behavior from the natural evolution of CASES-99 covariances. Previous attempts to reformulate surface layer equations, such as (3) and (4) or (6) and (7), have typically fit the mean fluxes so that they more closely fit the observed means or theoretically expected surface layer behavior. As we have shown, this approach does not always provide globally applicable formulas, nor does it account for the variability of natural events (particularly at high stability). A comprehensive representation of the global variability of surface layer evolution, including high dynamic stability and turbulence intermittency, would require far more extensive data than presented herein. A more appropriate dataset would consider geographic areas of widely varying physiographic characteristics and climatology, and different seasons and roughnesses, prior to determining a globally applicable mean behavior. We propose a more physically realistic approach to improve the standard deviation of the predicted flux values such that they represent the natural variability of the atmospheric fluxes. As shown in Figs. 4a and 5a, the data from a reasonably flat grass-

land in southeast Kansas show a much larger variability than represented by current surface layer schemes.

The data suggest that in addition to refitting the  $u_*$  and  $\theta_*$  relationships themselves [(3) and (4), or (6) and (7)] to more adequately capture the mean behavior at high  $Ri_b$  that a statistically bounded, physically based, stochastic component be added to the basic formulation of, say, (3), such that

$$\left\{ u_*^2 = \left[ \frac{k}{\ln\left(\frac{z}{z_0}\right)} \right]^2 \bar{U}^2 \left[ 1 + \frac{(10Ri_b)}{(1 + 5Ri_b)^{1/2}} \right]^{-1} + \varepsilon \right\},$$

$$Ri_b > 0, \quad (8)$$

where  $\varepsilon$  is a random variable within a defined probability function  $P$ ;  $P$  would be physically bounded by experimental data from measurements over a variety of surfaces around the globe for at least all four seasons. It is unrealistic to expect the CASES-99 field experiment data to adequately represent the characteristics of positive  $Ri_b$  behavior for the entire globe, as it is limited to the month of October, and a single surface characteristic. Furthermore,  $P$  would likely be a function of  $\Delta x$ ,  $\Delta y$ , and  $\Delta z$  (or  $z_1$ ); the grid spacings in  $x$ ,  $y$ , and  $z$ ;  $\Delta t$ , the numerical model integration time step; and  $D^2$ , the horizontal domain area of the particular model. Such a relationship is the focus of ongoing research, and is based on the inability of numerical models using discrete grid spacing and time steps to adequately represent the intermittency and even the existence of atmospheric phenomena responsible for fluxes in statically and dynamically stable conditions.

### 4. Summary

We have used CASES-99 nighttime observations to 1) calculate the sensible heat flux and  $u_*$  from two surface layer formulas (Louis et al. 1981; Delage 1997) and compare the parameterized fluxes to those observed; 2) investigate the "constant flux" assumption and the implications of that for the implementation of surface layer formulas; and 3) characterize the basic statistical behavior of heat and momentum fluxes for statically stable conditions, particularly large dynamic stability. Our results suggest that surface temperature numerical prediction errors, such as cold bias or occasional unrealistic cooling, over flat terrain can be ascribed to the inadequate representation of the impact of nonlocal NBL phenomena on local fluxes at high  $Ri_b$ , the placement of  $z_1$  at high levels compared to the actual surface layer height in the clear-sky NBL, and overprediction of cooling fluxes at relatively low  $Ri_b$ . We find that the Louis et al. (1981) and Delage (1997) formulas predict zero or near-zero sensible heat fluxes for all  $Ri_b > \sim 2.0$  and  $Ri_b > 1.0$ , respectively, whereas observations show considerable average negative heat flux for all  $Ri_b$ . For momentum flux, the Delage formula predicts near-zero

values for large  $Ri_b$ , while the Louis formula predicts more reasonable mean values. As a result cold air would be generated at the ground surface in a numerical model by radiational cooling, but not transferred to the first model grid level above ground, if model  $Ri_b$  became large. Thus, unrealistic vertical temperature gradients could be created that may not be adequately balanced by a radiative parameterization, or otherwise create numerical instability.

We have also investigated the constant flux assumption based on profiles of heat and momentum flux. Using a threshold value of 10% and we find that the average surface layer in the NBL for  $Ri_b > 0.2$  is either a few meters deep or undefined. These results suggest that it may be difficult to prescribe a fixed surface layer height in a numerical model, as is currently the practice, and to also expect exclusively similarity-based surface layer formulas to perform adequately at large stability. The near-surface heat fluxes were found, in the mean for  $Ri_b > 0.2$ , to be reasonably constant and nonmonotonic with height up to 55 m, making the boundary layer difficult to define, in part because of the influence of increasing intermittency between 20 and 55 m above ground. The  $u_*$  profile for  $Ri_b > 0.2$  was consistent with the upside-down boundary layer concept (Mahrt and Vickers 2002), making the surface layer undefinable, whereas the mean sensible heat flux profile exhibited a mirrored boundary layer shape.

We also found that the Louis et al. (1981) and Delage (1997) formulas overpredicted the magnitude of negative sensible heat flux for  $0.1 < Ri_b < 1.0$  and  $0.1 < Ri_b < 0.6$ , respectively, with this overprediction becoming worse and tending toward higher  $Ri_b$  with greater altitude. Momentum flux was also overpredicted by these formulas for most  $Ri_b < 0.5$ . As a result, at low but positive  $Ri_b$ , these formulas will transfer cool air at too great a rate to the first model grid point above ground. This behavior can lead to excessive cooling at  $z_1$  if flux divergence is negligible above the surface layer.

CASES-99 observations, as outlined in section 1 and indicated by the scatter, magnitude, and standard deviation of  $H$  and  $u_*$  for large  $Ri_b$ , clearly indicate a wide variety of nonlocal sources of potential mixing. Our results make it tempting to re-propose (Kondo et al. 1978) that the drag coefficient be a constant or nearly constant value for high  $Ri_b$ , allowing continued down-gradient transfer for all variables for  $Ri_b > 0$ . We propose instead a more physically realistic and comprehensive concept on the basis of the routine occurrence of various external atmospheric phenomena inducing fluxes. This approach introduces to surface layer formulas a random component of a defined probability function that would be physically bounded by far more comprehensive field observations and practically implemented with additional requirements based on model configuration.

*Acknowledgments.* Greg Poulos acknowledges the support of the ARO DAAD19-99-C-0037 and NSF ATM-0002093, and, for data analysis, this work was supported by the U.S. Department of Energy, under the auspices of the Environmental Meteorology Program of the Office of Biological and Environmental Research and DE-FG03-99ER62839. Sean Burns acknowledges the support of Army Research Office Grant DAAD 1999-1-0320 and National Science Foundation Grant ATM-9906637.

#### REFERENCES

- Acevedo, O. C., and D. R. Fitzjarrald, 2001: The early evening surface layer transition: Temporal and spatial variability. *J. Atmos. Sci.*, **58**, 2650–2667.
- , and —, 2003: In the core of the night—Effect of intermittent mixing on a horizontally heterogeneous surface. *Bound.-Layer Meteor.*, **106**, 1–33.
- Andreas, E. L., 2002: Parameterizing scalar transfer over snow and ice: A review. *J. Hydrometeor.*, **3**, 417–432.
- Arya, S. P. S., 1972: The critical condition for the maintenance of turbulence in stratified flows. *Quart. J. Roy. Meteor. Soc.*, **98**, 264–273.
- Banta, R. M., and P. T. Gannon Sr., 1995: Influence of soil moisture on simulation for katabatic flow. *Theor. Appl. Climatol.*, **52**, 84–94.
- , R. K. Newsom, J. K. Lundquist, Y. L. Pichugina, R. L. Coulter, and L. Mahrt, 2002: Nocturnal low-level jet characteristics over Kansas during CASES-99. *Bound.-Layer Meteor.*, **105**, 221–252.
- Barnard, J. C., 2000: Intermittent turbulence in the very stable Ekman layer. Ph.D. dissertation, University of Washington, 153 pp.
- Belair, S., P. Lacarrere, J. Noilhan, V. Masson, and J. Stein, 1998: High-resolution simulation of surface and turbulent fluxes during HAPEX-MOBILHY. *Mon. Wea. Rev.*, **126**, 2234–2253.
- Beljaars, A. C. M., and A. A. M. Holtslag, 1991: Flux parameterization over land surfaces for atmospheric models. *J. Appl. Meteor.*, **30**, 327–341.
- Bhumralkar, C. M., 1975: Numerical experiments on the computation of ground surface temperature in an atmospheric general circulation model. *J. Appl. Meteor.*, **14**, 1246–1258.
- Blumen, W., R. Banta, S. P. Burns, D. C. Fritts, R. Newsom, G. S. Poulos, and J. Sun, 2001: Turbulence statistics of a Kelvin–Helmholtz billow event observed in the nighttime boundary layer during the Cooperative Atmosphere–Surface Exchange Study field program. *Dyn. Atmos. Oceans*, **34**, 189–204.
- Businger, J. A., 1973: Turbulent transfer in the atmospheric surface layer. *Workshop on Micrometeorology*, D. H. Haugen, Ed., Amer. Meteor. Soc., 67–100.
- , J. C. Wyngaard, Y. Izumi, and E. F. Bradley, 1971: Flux-profile relationships in the atmospheric surface layer. *J. Atmos. Sci.*, **28**, 181–189.
- Carson, D. J., and P. J. R. Richards, 1978: Modelling surface turbulent fluxes in stable conditions. *Bound.-Layer Meteor.*, **14**, 68–81.
- Caughey, S. J., and C. J. Readings, 1975: An observation of waves and turbulence in the earth's boundary layer. *Bound.-Layer Meteor.*, **9**, 279–296.
- Chen, F., Z. Janjic, and K. Mitchell, 1997: Impact of atmospheric surface-layer parameterization in the new land-surface scheme of the NCEP mesoscale Eta Model. *Bound.-Layer Meteor.*, **85**, 391–421.
- Chimonas, G., 1985: Apparent counter-gradient heat fluxes generated by atmospheric wave. *Bound.-Layer Meteor.*, **31**, 1–12.
- Coulter, R., 1990: A case study of turbulence in the stable nocturnal boundary layer. *Bound.-Layer Meteor.*, **52**, 75–92.
- , and J. C. Doran, 2002: Spatial and temporal occurrences of intermittent turbulence during CASES-99. *Bound.-Layer Meteor.*, **105**, 329–349.

- De Baas, A. F., and A. G. M. Driedonks, 1985: Internal gravity waves in a stably stratified boundary layer. *Bound.-Layer Meteor.*, **31**, 303–323.
- Delage, Y., 1997: Parameterising sub-grid scale vertical transport in atmospheric models under statically stable conditions. *Bound.-Layer Meteor.*, **82**, 23–48.
- Derbyshire, S. H., 1994: A “balance” approach to stable boundary layer dynamics. *J. Atmos. Sci.*, **51**, 3486–3504.
- , 1995: Stable boundary layers: Observations, models and variability. Part I: Modeling and measurements. *Bound.-Layer Meteor.*, **74**, 19–54.
- , 1999: Boundary-layer decoupling over cold surfaces as a physical boundary instability. *Bound.-Layer Meteor.*, **90**, 297–325.
- Dubrulle, B., J.-P. Laval, and P. P. Sullivan, 2002a: A new dynamical subgrid model for the planetary surface layer. Part II: Analytical computation of fluxes, mean profiles, and variances. *J. Atmos. Sci.*, **59**, 877–891.
- , —, —, and J. Werne, 2002b: A new dynamical subgrid model for the planetary surface layer. Part I: The model and a priori tests. *J. Atmos. Sci.*, **59**, 861–876.
- Elliott, W. P., 1964: The height variation of vertical heat flux near the ground. *Quart. J. Roy. Meteor. Soc.*, **90**, 260–265.
- Ellison, T. H., 1957: Turbulent transport of heat and momentum from an infinite rough plate. *J. Fluid Mech.*, **2**, 456–466.
- Finnigan, J., 1979: Turbulence in waving wheat. *Bound.-Layer Meteor.*, **16**, 181–211.
- , 1999: A note on wave–turbulence interaction and the possibility of scaling the very stable boundary layer. *Bound.-Layer Meteor.*, **90**, 529–539.
- Fritts, D. C., C. Nappo, D. M. Riggan, B. B. Balsley, W. E. Eichinger, and R. K. Newsom, 2003: Analysis of ducted motions in the stable nocturnal boundary layer during CASES-99. *J. Atmos. Sci.*, **60**, 2450–2472.
- Funk, J. P., 1960: Measured radiative flux divergence near the ground at night. *Quart. J. Roy. Meteor. Soc.*, **86**, 382–389.
- Galmarini, S., C. Beets, P. G. Duynkerke, and J. Vila-Guerau de arellano, 1998: Stable nocturnal boundary layers: A comparison of one-dimensional and large eddy simulation models. *Bound.-Layer Meteor.*, **88**, 181–210.
- Hanna, S. R., and R. Yang, 2001: Evaluations of mesoscale models’ simulations of near-surface winds, temperature gradients, and mixing depths. *J. Appl. Meteor.*, **40**, 1095–1104.
- Hartel, C., and L. Kleiser, 1998: Analysis and modeling of subgrid-scale motions in near-wall turbulence. *J. Fluid Mech.*, **356**, 327–352.
- Herbert, F., and W.-G. Panhans, 1979: Theoretical studies of the parameterization of the non-neutral surface boundary layer. *Bound.-Layer Meteor.*, **16**, 155–167.
- Hill, R. J., 1997: Applicability of Kolmogorov’s and Monin’s equations of turbulence. *J. Fluid Mech.*, **353**, 67–81.
- Holtlag, A. A. M., and H. A. R. De Bruin, 1988: Applied modeling of the nighttime surface energy balance over land. *J. Appl. Meteor.*, **27**, 689–704.
- , and M. Ek, 1996: Simulation of surface fluxes and boundary layer development over the pine forest in HAPEX-MOBILHY. *J. Appl. Meteor.*, **35**, 202–213.
- Hooke, W. H., F. F. Hall, and E. E. Gossard, 1973: The observed generation of an atmospheric gravity wave by shear instability in the mean flow of the planetary boundary layer. *Bound.-Layer Meteor.*, **5**, 29–41.
- Howell, J., and L. Mahrt, 1997: Multiresolution flux decomposition. *Bound.-Layer Meteor.*, **83**, 117–137.
- , and J. Sun, 1997: Surface layer fluxes in stable conditions. *Bound.-Layer Meteor.*, **90**, 495–520.
- Hunt, J. C. R., G. J. Shutts, and S. H. Derbyshire, 1996: Stably stratified flows in meteorology. *Dyn. Atmos. Oceans*, **23**, 63–79.
- Katul, G. G., J. Albertson, M. Parlange, C.-R. Chu, and H. Stricker, 1994: Conditional sampling, bursting and the intermittent structure of sensible heat flux. *J. Geophys. Res.*, **99**, 22 869–22 876.
- Kim, J., and L. Mahrt, 1992: Simple formulation of turbulent mixing in the stable free atmosphere and nocturnal boundary layer. *Tellus*, **44A**, 381–394.
- Kondo, J., O. Kanechika, and N. Yasuda, 1978: Heat and momentum transfers under strong stability in the atmospheric surface layer. *J. Atmos. Sci.*, **35**, 1012–1021.
- Kosovic, B., and J. A. Curry, 2000: A large eddy simulation of quasi-steady, stably stratified atmospheric boundary layer. *J. Atmos. Sci.*, **57**, 1052–1068.
- Kot, S. C., and Y. Song, 1998: An improvement to the Louis scheme for the surface layer in an atmospheric modeling system. *Bound.-Layer Meteor.*, **88**, 239–254.
- Launiainen, J., 1995: Derivation of the relationship between the Obukhov stability parameter and the bulk Richardson number for flux-profile studies. *Bound.-Layer Meteor.*, **76**, 165–179.
- Louis, J. F., 1979: A parametric model of vertical eddy fluxes in the atmosphere. *Bound.-Layer Meteor.*, **17**, 187–202.
- , 1982: Parameterisation in weather prediction models. *Riv. Meteor. Aeronaut.*, **42**, 219–255.
- , M. Tiedtke, and J. F. Geleyn, 1981: A short history of the operational PBL parameterization at ECMWF. *Proc. Workshop on Planetary Boundary Layer Parameterization*, Reading, United Kingdom, ECMWF, 59–79.
- Mahrt, L., 1998a: Flux sampling errors for aircraft and towers. *J. Atmos. Oceanic Technol.*, **15**, 416–429.
- , 1998b: Stratified atmospheric boundary layers and breakdown of models. *J. Theor. Comput. Fluid Dyn.*, **11**, 263–280.
- , 1999: Stratified atmospheric boundary layer. *Bound.-Layer Meteor.*, **90**, 375–396.
- , and D. Vickers, 2002: Contrasting vertical structures of nocturnal boundary layers. *Bound.-Layer Meteor.*, **105**, 351–363.
- , J. Sun, W. Blumen, T. Delany, and S. Oncley, 1998: Nocturnal boundary-layer regimes. *Bound.-Layer Meteor.*, **88**, 255–278.
- McNider, R. T., D. E. England, M. J. Friedman, and X. Shi, 1995: Predictability of the stable atmospheric boundary layer. *J. Atmos. Sci.*, **52**, 1602–1623.
- McVehil, G. E., 1964: Wind and temperature profiles near the ground in stable stratification. *Quart. J. Roy. Meteor. Soc.*, **90**, 136–146.
- Monin, A. S., and A. M. Obukhov, 1954: Basic laws of turbulent mixing in the surface layer of the atmosphere. *Tr. Akad. Nauk SSSR Geofiz. Inst.*, **24**, 163–187.
- Nappo, C., 1991: Sporadic breakdowns of stability in the PBL over simple and complex terrain. *Bound.-Layer Meteor.*, **54**, 69–87.
- , and P.-E. Johansson, 1998: Summary report of the Lovanger international workshop on turbulence and diffusion in the stable planetary boundary layer. *Bull. Amer. Meteor. Soc.*, **79**, 1401–1405.
- Newsom, R. K., and R. M. Banta, 2003: Shear-flow instability in the stable nocturnal boundary layer as observed by Doppler lidar during CASES-99. *J. Atmos. Sci.*, **60**, 16–33.
- Nieuwstadt, F. T. M., 1984: Some aspects of the turbulent stable boundary layer. *Bound.-Layer Meteor.*, **30**, 31–55.
- Obukhov, A. M., 2001: *Turbulence and Atmospheric Dynamics*. Center for Turbulence Research Monogr., Stanford University Press, 514 pp.
- Oettl, D., R. A. Almbauer, and P. J. Sturm, 2001: A new method to estimate diffusion in stable, low-wind conditions. *J. Appl. Meteor.*, **40**, 259–268.
- Oke, T. R., 1970: Turbulent transport near the ground in stable conditions. *J. Appl. Meteor.*, **9**, 778–786.
- Panofsky, H. A., and J. A. Dutton, 1984: *Atmospheric Turbulence: Models and Methods for Engineering Applications*. John Wiley and Sons, 397 pp.
- Pielke, R. A., and Coauthors, 1992: A comprehensive meteorological modeling system—RAMS. *Meteor. Atmos. Phys.*, **49**, 69–91.
- Pleune, R., 1990: Vertical diffusion in the stable atmosphere. *Atmos. Environ.*, **24A**, 2547–2555.
- Poulos, G. S., 1996: The interaction of mountain waves and katabatic flows. Ph.D. dissertation, Colorado State University, 399 pp. [Available from Colorado State University, Dept. of Atmospheric Sciences, Fort Collins, CO 80523.]

- , and J. E. Bossert, 1995: An observational and prognostic numerical investigation of complex terrain dispersion. *J. Appl. Meteor.*, **34**, 650–669.
- , and Coauthors, 2002: CASES-99: A comprehensive investigation of the stable nocturnal boundary layer. *Bull. Amer. Meteor. Soc.*, **83**, 555–581.
- Revelle, D. O., 1993: Chaos and “bursting” in the planetary boundary layer. *J. Appl. Meteor.*, **32**, 1169–1180.
- Riley, J. J., and M.-P. Lelong, 2000: Fluid motions in the presence of strong stable stratification. *Annu. Rev. Fluid Mech.*, **32**, 613–657.
- Saiki, E. M., C.-H. Moeng, and P. P. Sullivan, 2000: Large eddy simulation of the stably stratified planetary boundary layer. *Bound.-Layer Meteor.*, **95**, 1–30.
- Schubert, J. F., 1977: Acoustic detection of momentum transfer during the abrupt transition from a laminar to a turbulent atmospheric boundary layer. *J. Appl. Meteor.*, **16**, 1292–1297.
- Soler, M. R., C. Infante, P. Buenestado, and L. Mahrt, 2002: Observations of nocturnal drainage flow in a shallow gully. *Bound.-Layer Meteor.*, **105**, 252–273.
- Sorbjan, Z., 1989: *Structure of the Atmospheric Boundary Layer*. Prentice Hall, 317 pp.
- Stewart, R. W., 1969: Turbulence and waves in a stratified atmosphere. *Radio Sci.*, **4**, 1269–1278.
- Sun, J., and Coauthors, 2002: Intermittent turbulence associated with a density current passage in the stable boundary layer. *Bound.-Layer Meteor.*, **105**, 199–219.
- Thorpe, A. J., and T. H. Guymer, 1977: The nocturnal jet. *Quart. J. Roy. Meteor. Soc.*, **103**, 633–653.
- van den Hurk, B. J. J. M., and A. A. M. Holtslag, 1997: On the bulk parameterization of surface layer fluxes for various conditions and parameter ranges. *Bound.-Layer Meteor.*, **82**, 119–134.
- van de Wiel, B. J. H., A. F. Moene, R. J. Ronda, H. A. R. De Bruin, and A. A. M. Holtslag, 2002a: Intermittent turbulence and oscillations in the stable boundary layer over land. Part II: A system dynamics approach. *J. Atmos. Sci.*, **59**, 2567–2581.
- , R. J. Ronda, A. F. Moene, H. A. R. De Bruin, and A. A. M. Holtslag, 2002b: Intermittent turbulence and oscillations in the stable boundary layer over land. Part I: A bulk model. *J. Atmos. Sci.*, **59**, 942–958.
- Viterbo, P., A. Beljaars, J.-F. Mahfouf, and J. Teixeira, 1999: The representation of soil moisture freezing and its impact on the stable boundary layer. *Quart. J. Roy. Meteor. Soc.*, **125**, 2401–2426.
- Webb, E. K., 1970: Profile relationships: The log-linear range and extension to strong stability. *Quart. J. Roy. Meteor. Soc.*, **96**, 67–90.
- Weber, A. H., and R. J. Kurzeja, 1991: Nocturnal planetary boundary layer structure and turbulence episodes during the Project STABLE field program. *J. Appl. Meteor.*, **30**, 1117–1133.
- Werne, J., and D. C. Fritts, 1999: Stratified shear turbulence: Evolution and statistics. *Geophys. Res. Lett.*, **26**, 439–442.
- , and —, 2001: Anisotropy in a stratified shear layer. *Phys. Chem. Earth*, **26B**, 263–268.
- Woods, J. D., 1969: On Richardson’s number as a criterion for laminar–turbulent–laminar transition in the ocean and atmosphere. *Radio Sci.*, **4**, 1289–1298.
- Wyngaard, J. C., 1975: Modeling the planetary boundary layer—Extension to the stable case. *Bound.-Layer Meteor.*, **9**, 441–460.
- , and L. J. Peltier, 1996: Experimental micrometeorology in an era of turbulence simulation. *Bound.-Layer Meteor.*, **78**, 71–86.
- Yaglom, A. M., 1977: Comments on wind and temperature flux–profile relationships. *Bound.-Layer Meteor.*, **11**, 89–102.
- Yamada, T., 1975: The critical Richardson number and the ratio of the eddy transport coefficients obtained from a turbulence closure model. *J. Atmos. Sci.*, **32**, 926–933.